Effects of Mutation of the Conserved Glutamic Acid-286 in Subunit I of Cytochrome *c* Oxidase from *Rhodobacter sphaeroides*†

Susanne Jünemann,* Brigitte Meunier, Nicholas Fisher, and Peter R. Rich

Glynn Laboratory of Bioenergetics, Department of Biology, University College, Gower Street, London, WC1E 6BT, U.K.

Received December 22, 1998; Revised Manuscript Received March 2, 1999

ABSTRACT: We have studied the effects of mutations, E286Q and E286D, of the conserved glutamate in subunit I of cytochrome *c* oxidase from *Rhodobacter sphaeroides* with a view to evaluating the role of this residue in redox-linked proton translocation. The mutation E286D did not have any dramatic effects on enzyme properties and retained 50% of wild-type catalytic activity. For E286Q a fraction of the binuclear center was trapped in an unreactive, spectrally distinct form which is most likely due to misfolded protein, but the majority of E286Q reacted normally with formate and cyanide in the oxidized state, and with carbon monoxide and cyanide in the dithionite-reduced form. The mutation also had little effect on the pH-dependent redox properties of haem *a* in the reactive fraction. However, formation of the **P** state from oxidized enzyme with hydrogen peroxide or by aerobic incubation with carbon monoxide was inhibited. In particular, only an **F**-type product was obtained, at less than 25% yield, in the reaction with hydrogen peroxide. The aerobic steady state in the presence of ferrous cytochrome *c* was characterized by essentially fully reduced haem *a* and ferric haem a_3, suggesting that the mutation hinders electron transfer from haem *a* to the binuclear center. Under these conditions or after reoxidation, on a seconds time scale, of haem a_3 following anaerobiosis, there was no indication of accumulation of significant amounts of **P** state. We propose that the glutamate is implicated in several steps in the catalytic cycle, **O** → **R**, **P** → **F**, and, possibly, **F** → **O**. The results are discussed in relation to the "glutamate trap" model for proton translocation.

Although two structures of cytochrome oxidase have been published (*1*, *2*) and extensive information has been gained on the number and nature of intermediates in the catalytic cycle of oxygen reduction to water (reviewed in ref *3*), the mechanism by which electron transfer is coupled to proton translocation across the membrane remains unresolved. The catalytic cycle starts with reduction of the oxidized form of the binuclear center, termed **O**,[1] with two electrons to form the **R** state which can react with oxygen to produce the "peroxy" intermediate **P**. Input of a third electron converts **P** to the "ferryl" intermediate **F**. This in turn returns to the **O** state on input of a fourth electron.

The energy cost of introducing a charge, such as an electron, into the binuclear center of cytochrome *c* oxidase is lowered by associated binding of protons to appropriately placed residues (*4*, *5*). Each catalytic cycle is associated with uptake from the N-aqueous phase of four "substrate" protons, H^+_S, which are required for water formation, and four "pumped" protons, H^+_T, which are transferred across the membrane to the P-aqueous phase. Only the **P** → **F** → **O** steps have been thought to be associated with net proton pumping, although this conclusion has been questioned recently (*6*). Clearly, the understanding of the chemistry of the charge-linked protonation processes is crucial to understanding the mechanism of proton pumping. Site-directed mutagenesis studies (*7*, *8*) and the crystal structures of cytochrome oxidase from *Paracoccus denitrificans* (*1*) and bovine heart (*2*) have identified possible protonation sites and routes in subunit I. Candidates for charge-linked protonation sites include the conserved glutamate-286 (in *Rhodobacter sphaeroides* numbering), a residue that is close to haem *a* and the binuclear center metals and appears to be at the end of "pore A", one of the two predicted proton pathways. Mutation of E286 can lead to a dramatic loss of catalytic activity and associated proton pumping (reviewed in ref *9*). More specifically, flow-flash experiments were used to demonstrate that the reaction of fully reduced E286A or Q mutants with oxygen can proceed only partially, to the **P** state, and without uptake of protons from the medium (*10*−*12*). A study of the time-resolved generation of membrane potential points to a requirement for the glutamate in the **F** → **O** transition (*13*). It has also been shown that the "peroxidase half-reaction" of the oxidase, that is, the H_2O_2 and ferrocytochrome *c* driven cycle of **O** → **P** → **F** → **O**, is not functional in the E286Q mutant (*14*, *15*). These data support a crucial function for E286 and its associated pore A in proton translocation, although their precise role during the catalytic cycle is less clear. Since the second putative

† This work is funded by grants from the Wellcome Trust (to P.R.R., Grant no. 049722/2/96/2 PMG/RC) and HFSP (to P.R.R., grant no. RG-464/95M) and a MRC Career Development Award (to B.M.).

* Corresponding author. Tel/Fax: +44 171 380 7746. E-mail s.junemann@ucl.ac.uk.

[1] Abbreviations: CO, carbon monoxide; E_h, redox potential; E_m, midpoint potential; **O**, **R**, **P**, and **F**, oxidized, two-electron reduced, peroxy, and ferryl intermediates of cytochrome oxidase; NTA, nitrilotriacetic acid; H^+_S, substrate protons; H^+_T, pumped protons; FTIR, Fourier transform infrared; TMPD, *N*,*N*,*N*′,*N*′-tetramethyl-*p*-phenylenediamine.

10.1021/bi9830112 CCC: $18.00
Published on Web 04/02/1999

proton channel, "pore B", appears to lead from the N-phase to the binuclear center and is thus a good candidate for transfer of substrate protons (H^+_S), it had initially been suggested (*1*) that pores A and B convey exclusively H^+_T and H^+_S, respectively. However, this view has been questioned on the basis of work on mutations of K362, a central residue in pore B, where the most striking effect is an inhibition of the **O** to **R** step (*16*, *17*). Alternative working models suggest that pore B might act as a "dielectric well" instead of a proton channel (*16*) or that the two proton channels may not conduct exclusively H^+_S or H^+_T but may change their role at different stages of the catalytic cycle (*13*).

In this paper, we describe the effects of two mutations of glutamate-286 in cytochrome *c* oxidase from *Rhodobacter sphaeroides*, E286Q and E286D. We have previously studied a preparation of the E286Q mutant where 80−90% of the binuclear center was trapped in a ligand and redox-unreactive state (*9*). New preparations of E286Q have now been made in our laboratory. In these samples the enzyme was predominantly in a reactive form, allowing further characterization of individual electron and proton-transfer reactions. We have applied a set of diagnostic tests, including redox properties, ligand reactivity, and steady-state behavior, which was originally designed for a similar study of the role of the conserved lysine-362 (*16*). The function of E286, as assessed by these tests, is discussed in relation to the mechanism of coupling proton and electron transfer.

MATERIALS AND METHODS

Growth of Organism and Preparation of Enzymes. His-tagged forms of wild-type and mutant cytochrome *c* oxidase from *R. sphaeroides* were produced as described in ref *18*. After elution of the oxidase from the Ni^{2+}-NTA column (*18*), the buffer was exchanged by 50 mM Tricine, pH 8.5, 0.1% (w/v) lauryl maltoside by repeated cycles of ultrafiltration in Centriprep 10 units (Amicon). Glycerol (5% w/v) was added prior to storage at −70 °C.

Since the optical spectra of wild-type cytochrome *c* oxidase from *R. sphaeroides* are very similar to those of the bovine enzyme (*19*), extinction coefficients for the latter (*20*) were used to quantitate the levels of reduced, oxidized, and various ligand-bound states of the wild-type *R. sphaeroides* oxidase (cf. ref *16*). The same extinction coefficients were used for the mutant enzymes after adjustment of wavelengths where necessary, as indicated in the text. In particular, quantitation of oxidase was based on the dithionite-reduced *minus* ferricyanide-oxidized difference spectrum, using $\epsilon = 25$ mM^{-1} cm^{-1} at 606 *minus* 620 nm (*20*).

Optical Spectroscopy and Kinetic Measurements. Optical spectra and multiwavelength kinetics were monitored at room temperature in the same sample using a single-beam instrument built in-house. Actinic light pulses for photolysis of the ferrous CO and cyanide compounds of the oxidase were provided by a frequency-doubled Nd:YAG laser (10 ns halfpeak width, 532 nm, >100 mJ/pulse; Spectron Ltd., Rugby, UK) or by a commercial xenon flashlamp (1 ms halfpeak width, 125 V working voltage; Bauer).

Potentiometric Titrations. Anaerobic redox titrations were carried out in 2 mL of 50 mM potassium phosphate, 0.1% lauryl maltoside, 2 mM cyanide at different pH values.

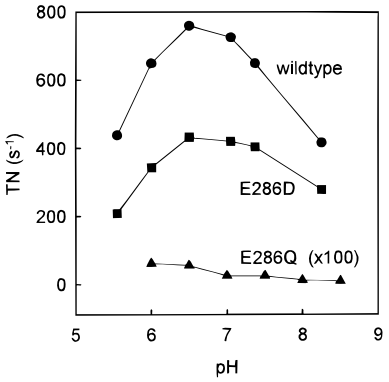

FIGURE 1: Catalytic activity of the wild-type and mutant enzymes. Oxygen consumption was measured at room temperature in a Clark-type oxygen electrode in a medium containing 50 mM potassium phosphate, 0.1% lauryl maltoside, 10 mM ascorbate, 50 μM TMPD, and 60 μM cytochrome *c* at different pH values. The reaction was initiated by the addition of appropriate amounts of wild-type or mutant oxidase.

Purified cytochrome *c* oxidase was added to around 1 μM, and the mixture was kept anaerobic with a positive pressure of argon above the liquid surface. Redox mediators were the following (E_m in mV, concentration in μM): phenazine methosulfate (+80, 8); 2,6-dichlorophenolindophenol (+220, 15); TMPD (+275, 50); ferricyanide (+440, 50); 1,2-naphthoquinone-4-sulfonate (+215, 5); 1,2-naphthoquinone (+143, 5); 1,4-benzoquinone (+293, 50); 2,6-dimethyl-1,4-benzoquinone (168, 40); methyl-hydroquinone (+224, 40); cytochrome *c* (+255, 3). Potassium ascorbate (20 mM stock solution) was used as reductant, and potassium permanganate (10 mM stock solution) was used as oxidant. Redox potentials were measured in the stirred sample with a platinum electrode and a Ag/AgCl reference electrode. After stabilization of the potential, stirring was stopped and the spectrum between 390 and 490 nm was recorded. To minimize interference from redox dyes or baseline drift, we derived titration curves from triple wavelength measurements at 445 nm − (435 nm + 455 nm)/2 nm. The data represent points taken in both oxidative and reductive directions.

RESULTS

Effects of Mutations on Catalytic Activity. Figure 1 compares the cytochrome *c* oxidase activities of wild type and two mutant enzymes, E286Q and E286D, as measured in an oxygen electrode. While replacement of glutamate-286 by the protonatable aspartate results in an enzyme that retains at least 50% of the wild-type activity, replacement by the nonprotonatable glutamine abolishes turnover almost completely (turnover < 1 s^{-1}), consistent with previous reports on the *R. sphaeroides* mutants and their equivalents in the *bo*-type oxidase from *Escherichia coli* (*21*, *22*). While the pH dependency of E286D turnover parallels that of the wild type, the turnover number of E286Q increases from around 0.1 s^{-1} at pH 8.5 to around 0.6 s^{-1} at pH 6 with no clear pH optimum.

Analysis of the "As Prepared" State. Absolute optical spectra of wild-type and E286Q mutant oxidase, as prepared, are presented in Figure 2. The position of the Soret peak at 425 nm (α-band near 600 nm) and the Soret/α-band ratio of 6.7 indicate that, under these conditions, the wild-type enzyme (inset to panel A) is essentially fully oxidized (cf.

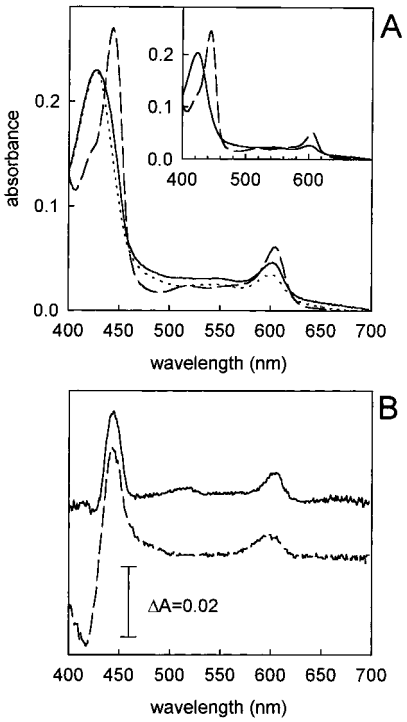

FIGURE 2: Optical spectra of the wild-type and E286Q mutant cytochrome *c* oxidase. Oxidase samples were diluted to around 1 μM in 0.5 mL of 50 mM potassium phosphate, 0.05% lauryl maltoside, pH 7.5. Ferricyanide (100 μM) was used as an oxidant, and oxidation was judged to be complete when no further spectral changes could be detected. (A) E286Q as prepared (—), ferricyanide-oxidized (•••), and dithionite-reduced (---) absolute spectra; the inset shows wild type as prepared (—) and dithionite-reduced (---) absolute spectra. (B) E286Q as prepared *minus* oxidized (—) and oxidized E286Q *minus* oxidized wild-type (---) difference spectra.

refs *16*, *20*), as is also the case in E286D mutant preparations (not shown). In contrast, a sample of E286Q mutant enzyme (panel A) shows the Soret peak at 426 nm with a shoulder on the red side and a comparatively intense α-band at 605 nm (Soret/α-band ratio of 4.9). These features are partly due to the presence of some ferricyanide-oxidizable component (panel B). This has a spectrum characteristic of haem *a* (cf. ref *16*) and quantitates to 30% of the total haem *a*, using an extinction coefficient of 18.6 mM^{-1} cm^{-1} at 606−621 nm (*23*). However, the position of the Soret peak in the absolute oxidized spectrum at 425−426 nm is still higher that in the wild type (423−424 nm), and the α-band is slightly broader. Subtracting appropriate amounts of the spectrum of oxidized wild-type enzyme from that of oxidized E286Q (panel B) reveals a species in the E286Q preparation which we have termed the "595 nm form" after the position of its α-peak in the oxidized E286Q *minus* oxidized wild-type difference spectrum. The 595 nm form is further characterized by a Soret band redshifted compared to oxidized wild-type enzyme, thus giving rise to the spectral distortions found in ferricyanide-treated E286Q oxidase. The compound is redox-inactive in that it can still be detected in the (reduced E286Q) *minus* (reduced wild type) difference spectrum after 20 min of incubation with dithionite (not shown).

Binding of Ligands to the Ferric Enzyme. Formate, cyanide, hydrogen peroxide, and carbon monoxide were used to assess ligand reactivity of the ferricyanide-oxidized forms (Table 1). Reaction of both E286 mutants with formate and cyanide gave normal binding spectra (cf. refs *16*, *20*) and rate constants comparable to those of the wild type. While the extent of reaction was close to stoichiometric in the E286D mutant, E286Q oxidase showed a lowered yield with only 70% formation of the cyanide or formate compounds. We conclude that the major population of the E286Q mutant had a fully oxidized binuclear center since formate binds only when haem a_3 and Cu_B are both oxidized (*24*), while around 30% did not react with ligands at all.

Table 1: Reactivity with Ligands in Various Redox States[a]

	extent of reaction [b] (rate constant)		
	wild type	E286Q	E286D
Composition of As Prepared Enzyme			
oxidized	100%		≥95%
haem *a* reduced		30%	≤5%
other		30% 595 form	
Reactivity of Ferricyanide-Treated Enzyme			
cyanide (10 mM)	100% (0.025 s^{-1})	70% (0.012 s^{-1})	95% (0.035 s^{-1})
formate (25 mM)	99%	70%	95%
H_2O_2 (50 μM − 1 mM, at pH 6.5 and 8.5)	94%	≤28% (only **F**-type)	96%
CO (1 mM at pH 8.5)	92%	≤25% (not **P**)	55%
Reactivity of Dithionite-Reduced Enzyme			
CO (1 mM)	100% (50 s^{-1})	60−70% (50 s^{-1})[c]	100% (50 s^{-1})
cyanide (10 mM)	85−100% (7 s^{-1})	60−70% (4 s^{-1})[c]	95% (7 s^{-1})

[a] Experiments were carried out in 50 mM potassium phosphate buffer, pH 7.5, containing 0.05% (w/v) lauryl maltoside, unless otherwise indicated. [b] The extent of ligated form was calculated from the difference spectra compared to the signal expected for 100% reactivity, based on the extinction coefficients in ref *16*. [c] The kinetics were biphasic with 15% of a factor of 3 slower phases.

Incubation of cytochrome oxidase with H_2O_2 leads to formation of **P** and at least two **F**-type species, **F** and **F•**, with the relative amounts of these products dependent mainly on pH and H_2O_2 concentration (*25*, *26*). The kinetics of these reactions have been resolved for the *bo*-type oxidase from *E. coli* (*26*) and bovine heart oxidase (Jünemann and Rich, unpublished results). Kinetic analysis of the reaction of cytochrome oxidase from *R. sphaeroides* has given rate constants similar to those of the bovine enzyme (not shown). On this basis, H_2O_2 reactivity of the mutants was probed over a range of ligand concentrations (50 μM to 1 mM) and pH values (6.5−8.5). While the E286D enzyme reacts normally with regard to yield, product ratios, and kinetics (not shown), reaction of the E286Q form is severely impaired (Table 1 and Figure 3A), with a reduction in yield to between 10% and 25%. The product is entirely a 580 nm species in the pH range 6.5−8.5, although it was not possible to determine whether this was **F** or **F•** due to low signal intensity. No **P** is detected either at equilibrium (Figure 3A) or as a transient species (not shown). Despite this difference, the kinetics of interaction of oxidized E286Q with the first H_2O_2 molecule, as monitored at 436 *minus* 416 nm, are similar to those of the wild type (approximately 400 M^{-1} s^{-1}).

Two-electron reduction of fully oxidized enzyme with CO results in a mixed-valence form (*27*) which, under aerobic conditions, then reacts with oxygen to form the **P** state. At alkaline pH, over 90% of the wild-type enzyme can be converted to **P** (Figure 3B) within 15 min. The reaction of

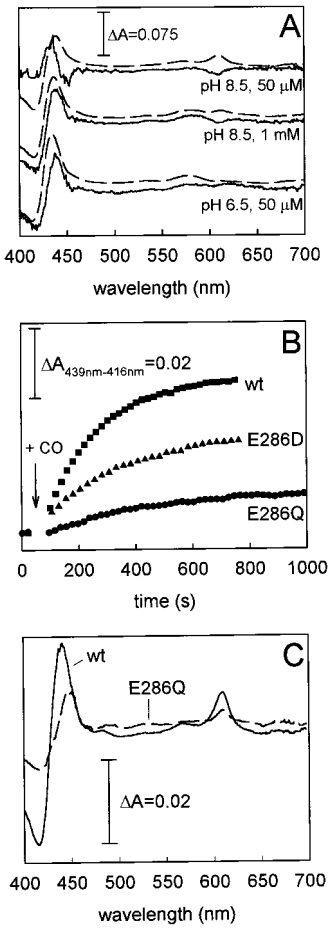

FIGURE 3: Formation of the **P** state by different methods. Oxidase samples (1 μM) were suspended in 0.5 mL of 50 mM potassium phosphate, 100 μM ferricyanide, 0.05% lauryl maltoside. (A) E286Q (—) and wild-type (---) difference spectra versus the oxidized form following incubation with H_2O_2 at the concentration and pH indicated. Note that the wild-type spectra are reduced by a factor of 5. (B) Progress curves at 439 *minus* 416 nm and (C) difference spectra versus the oxidized form following bubbling with CO at pH 8.5 under aerobic conditions.

E286Q is slower, and with less than 25% final yield, as shown in Figure 3B,C. Furthermore, the position of the Soret peak at 447 nm in the difference spectrum versus the oxidized form (Figure 3C) is not typical of **P** but instead suggests some formation of reduced haem *a*. The same spectrum is obtained by anaerobic incubation of E286Q with CO, indicating that the mutation prevents formation of the **R** state with CO in the reductive step. The CO/O_2 reaction is also impaired, to a lesser degree, in the E286D mutant, where the yield of the **P** state does not exceed 55% (not shown).

Reaction of the Dithionite-Reduced Enzyme. Reduced E286 mutant oxidases were prepared from as prepared or ferricyanide-oxidized samples by the addition of dithionite. Reduced E286Q *minus* reduced wild-type difference spectra (not shown) indicate that this treatment leads to the reduction of haem *a* and of that fraction of haem a_3 (70%) which is not in the 595 nm form. The 595 nm form remains redox-unreactive over at least 30 min. Reduction kinetics of the E286Q enzyme, monitored at the wavelength pairs 606−621 nm and 447−462 nm, are similar to those of the wild type (half-time of less than 4 s, not shown).

Reaction of dithionite-reduced enzyme with CO and cyanide was used to probe heterogeneity and ligand-linked

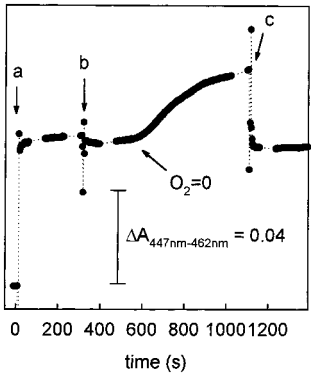

FIGURE 4: Steady-state behavior of E286Q mutant oxidase. The E286Q enzyme was dissolved to 1 μM in 50 mM potassium phosphate, 0.1% lauryl maltoside, pH 7.5. Steady-state redox changes of the haems monitored at 447−462 nm where the spectral contributions of cytochrome *c* are negligible. The following additions were made: (a) 1.6 μM cytochrome *c*, 10 mM ascorbate, and 10 μM TMPD; (b) 10 mM glucose, 5 units/mL glucose oxidase, and 50 units/mL catalase.

proton uptake (cf. ref *16*). Both E286 mutant oxidases give normal binding spectra, although the extent of reaction is only 70% (of the total enzyme population) in E286Q oxidase (Table 1), consistent with a fraction of 30% of the enzyme which cannot be reduced by dithionite. CO or cyanide recombination kinetics are as in wild type, except for a minor fraction (15%, Table 1) in E286Q preparations where a slower recombination rate constant indicates a further heterogeneity problem.

Steady State. In the experiment shown in Figures 4 and 5 low levels of reductant (cytochrome *c* plus ascorbate and TMPD, at pH 7.5) were used to assess the behavior of the E286Q oxidase in the aerobic steady state. Following the addition of substrate, a steady state is reached within seconds. The difference spectrum of this state (Figure 5A, trace a) has maxima at 607 and 447 nm with a Soret (447−462 nm)/α-band (607−621 nm) ratio of 3.8, characteristic of reduced haem *a* (compare 3.6 for wild-type haem *a* reduced *minus* oxidized spectrum Figure 5B, trace b). With an extinction coefficient of $\Delta\epsilon$(607−621 nm) = 18.6 mM^{-1} cm^{-1} (*23*) this can be quantitated to 60−65% of the total haem *a* (plus 30% which is already reduced in as prepared samples). Features indicative of the oxygen intermediates **P** (lower Soret peak position and lower Soret/α-band ratio, cf. Figure 3A) or **F** (distinctive band near 580 nm) are absent. These intermediates could not be detected at more acidic or alkaline pH (6.5 or 8.5, not shown). The cytochrome *c* reduction level in the E286Q sample is 80−90%. We have reported previously (*16*, *28*) that the same steady state of wild-type enzyme is characterized by only partial haem *a* reduction (30−40%) and the presence of some oxygen intermediates (30−40%, mostly **F**), with no more than 10% reduced cytochrome *c*.

Due to the low activity of the E286Q enzyme, glucose/glucose oxidase/catalase were used to induce anaerobiosis. The absorbance increase at 447 *minus* 462 nm following oxygen depletion (Figure 4) can be ascribed to the reduction of haem a_3 (70% of the total oxidase, using $\Delta\epsilon$(447−463 nm) = 82.3 mM^{-1} cm^{-1} (*23*)) and the remainder of haem *a*, as shown by the anaerobic *minus* steady state difference spectrum (Figure 5A, trace b, cf. Figure 5B, trace a).

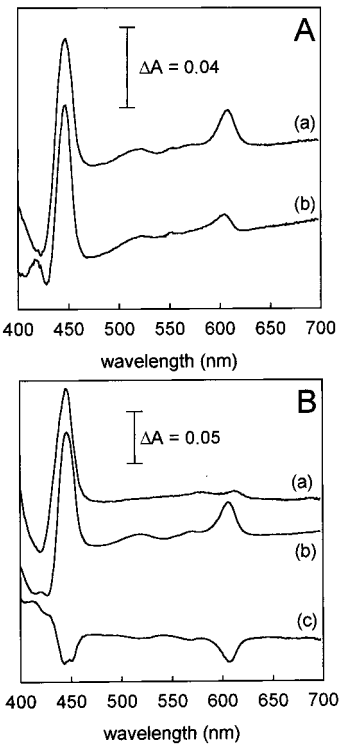

FIGURE 5: Steady-state spectra of E286Q mutant oxidase. (A) Steady-state spectra of E286Q were recorded during the real time experiment shown in Figure 4 in the same sample. Spectral contributions of cytochrome *c* have been subtracted: (a) (after oxygen pulse) *minus* (as prepared), (b) (anaerobic) *minus* (aerobic steady state). (B) For comparison the following wild-type spectra were recorded (1 μM enzyme in 50 mM potassium phosphate, 0.1% lauryl maltoside, pH 7.5): (a) haem a_3 reduced *minus* oxidized, obtained by subtracting spectrum (b) from dithionite-reduced enzyme; (b) haem *a* reduced *minus* oxidized, obtained by reduction of the cyanide-ligated enzyme with 5 mM dithionite; and (c) reduced haem a_3 *minus* **P**. **P** was obtained by the CO/O_2 method (see text), and the spectrum was calculated as (dithionite-reduced) *minus* (**P**+ spectrum (b)).

An oxygen pulse given to the anaerobic sample causes reoxidation back to the aerobic steady state (Figure 4) with a spectrum identical to that before anaerobiosis (Figure 5A, trace a). In particular, comparison of the anaerobic *minus* (after oxygen pulse) difference spectrum with a calculated ($a^{2+}a_3^{2+}$) *minus* (a^{2+}**P**) difference spectrum (Figure 5B, trace c) shows that, on a seconds time scale, **P** is not accumulated following reaction of fully reduced E286Q enzyme with oxygen.

Reaction with Formate in the Steady State. The reaction with formate in the presence of low levels of reduced cytochrome *c* was used to probe the reduction state of the binuclear center of E286Q enzyme in the aerobic steady state.

The steady-state formate-binding spectrum of E286Q, given in Figure 6, trace b, shows a peak and trough at 415 and 432 nm, respectively, indicative of the interaction of formate with a fully oxidized binuclear center, together with peaks at 447 and 607 nm due to further haem *a* reduction. The experimental conditions were such that in the initial steady state the haem *a* reduction level was 75%, with spectral features otherwise identical to those shown in Figure 5. The addition of formate leads to the reduction of the remaining 25% of haem *a*. The subtraction of the spectral contribution of haem *a* using the wild-type spectrum of Figure 5B, trace b, shows quantitative formate binding of

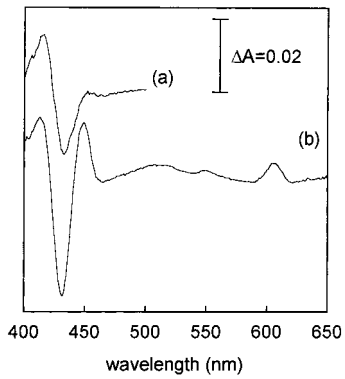

FIGURE 6: Reaction with formate in the aerobic steady state. Oxidase samples were dissolved to 1 μM in 50 mM potassium phosphate, 0.1% lauryl maltoside, pH 7.5. The steady state was established as in Figure 4, except for a lower cytochrome *c* concentration of 0.03 μM, and 25 mM formate were added. For comparison, trace (a) shows the formate-binding spectrum of ferricyanide-oxidized E286Q.

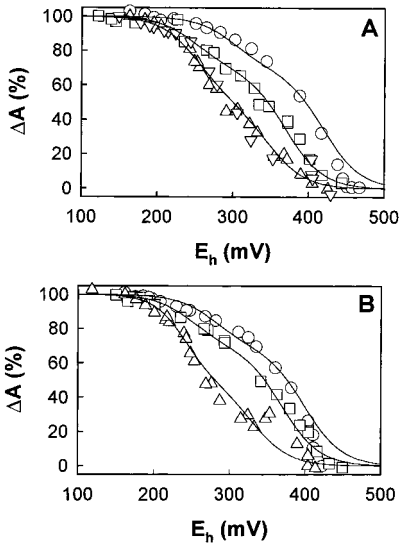

FIGURE 7: Midpoint potentials of cyanide-ligated wild-type and E286Q mutant oxidase. Redox titrations were performed as described in Materials and Methods. The data points are overlaid with calculated traces based on a model of anticooperative interaction between haem *a* and Cu_B (*29*), as described in the main text. Titrations of wild-type (A) and E286Q mutant oxidase (B) were carried out at pH 6.5 (○), 7.5 (□), and 8.9 (△).

the reactive proportion of the binuclear center (70−80%). Spectral features very similar to those shown in Figure 6b have been obtained in an identical experiment with wild-type enzyme (*16*), equivalent to 70% formate binding plus 50% extra haem *a* reduction.

Effect of Mutation on Redox Potentials. Redox titrations of haem *a* in cyanide-ligated enzyme are presented in Figure 7. For the wild-type form (Figure 7A), titration curves with midpoints at 395, 350, and 300 mV are obtained at pH 6.5, 7.5, and 8.9, respectively. The distortion from an $n = 1$ shape can be ascribed to the interaction of haem *a* with the other redox centers. Simulations based on a model (*29*) of anticooperative interaction between haem *a* and Cu_B, but without taking account of any weak interaction with Cu_A, yield microscopic E_m values of haem *a* (i.e., midpoint potentials of haem *a* with Cu_B either reduced or oxidized) and estimates for the microscopic E_m values of Cu_B (data not shown). The potentials decrease by around −40 mV/pH

unit due to haem *a* redox-linked protonation processes, similar to values obtained with mammalian and yeast enzymes (*29*, *30*).

The E286Q mutation has little effect on the haem *a* (and Cu_B) midpoint potentials. Titration curves at pH 6.5, 7.5, and 8.9 had observed midpoints at 380, 350, and 280 mV, respectively, and retained the Cu_B induced distortions (Figure 7B), with the microscopic E_m values close to wild-type values (not shown).

DISCUSSION

Heterogeneity. The reactivity of a typical preparation of oxidized or reduced E286Q oxidase toward a number of ligands was normal for the major population (60−70%), while the remainder was unreactive. We suggest that the unreactive fraction can be entirely accounted for by a 595 nm form, as revealed in E286Q *minus* wild-type difference spectra (Figure 2B). The amount of this 595 nm form in different preparations varies, and this is reflected in proportionally decreased ligand reactivity. For example, the first E286Q preparation analyzed in this laboratory contained less than 15% reactive enzyme with over 85% trapped in the ligand- and redox-unreactive 595 nm form (*9*). By using a preparation such as described in Table 1 (30% unreactive), we have estimated an extinction coefficient for the 595 nm form of 4−8 mM^{-1} cm^{-1} (595 *minus* 620 nm, E286 *minus* wild type). While spectrally similar to compound A (the species produced transiently on binding of oxygen to ferrous haem a_3 (*31*, *32*)), the 595 nm form is not photolabile, unlike compound A (*33*), and is of unknown origin. Although it has been noted that the imidazole used to elute his-tagged oxidase from the Ni−NTA column may lead to slight changes in the optical spectrum (*34*), the 595 nm form is unlikely to be a preparation artifact as it is present in membrane samples before solubilization (spectra not shown) and is partially removed by further purification steps. This suggests that the 595 nm form arises from some misfolding of the mutant protein, leading to solubilization properties and/or accessibility of the his-tag different from correctly folded oxidase. It should be noted that quantitation of the oxidase was based on the α-band at 606 *minus* 621 nm (see Materials and Methods). As haem a_3 contributes only about 20% to this signal (*23*) the quantitation error caused by the 595 nm form will be small.

The "reactive" population of the enzyme which is not trapped in the 595 nm form (around 70%) was itself found be heterogeneous in that CO and cyanide recombination to the ferrous enzyme following photolysis showed biphasic kinetics with 15% of a slow phase. Otherwise, however, most ligand reactions (except those involving **P** formation, see below) were normal in both mutants, indicating that the redox centers, in particular the binuclear center, are intact.

pH Dependency of E_m of Haem a and Cu_B. The data in Figure 7 show that in the pH range 6.5−8.9 the E286Q mutation has very little effect on redox titrations of haem *a* in the cyanide-ligated form of the reactive fraction of the enzyme. In particular, the titration curves retain the distortion from a simple $n = 1$ shape which has been ascribed to anticooperative redox interaction between haem *a* and Cu_B mediated by at least two protonatable groups with different p*K* values (*29*). Since the redox potentials of haem *a* and Cu_B, their interaction, and pH dependencies are not significantly altered in the E286Q mutant, we conclude that the residue E286 cannot be one of the major protonatable groups redox-linked to haem *a*. This conclusion is in agreement with the suggestion, based on FTIR measurements, that E286 is always in the protonated state (*35*).

We have previously studied a yeast cytochrome oxidase mutant where an asparagine was introduced in place of isoleucine-67, a residue located in the vicinity of the conserved glutamate-243 (the equivalent to E286 in *R. sphaeroides*). In this I67N enzyme the haem *a* midpoint potential was lowered by 55 mV at pH 7.5 and its pH dependency was weakened. This was interpreted as the I67N mutation perturbing, possibly by introducing a new hydrogen bond, the protonation properties of the conserved glutamate which in turn would be redox-linked to haem *a* and affect its E_m (*30*, *36*). In light of the present data this interpretation needs to be reconsidered. One possibility is that the observed E_m changes are due to more direct effects of the I67N mutation on haem *a* which are not mediated by E243. Interaction between I67 and E243 might be similar to that in the *Paracoccus denitrificans* oxidase where the equivalent residues M99 and E286 are connected via a water molecule (*37*). In this case, the severe inhibition of turnover caused by mutation of I67 might arise from changes in mobility and local structure around E286, as well as from the effects on the E_m of haem *a*.

*Generation of **P** from the Ferricyanide-Treated Form*. While most ligand reactions of the E286Q mutant summarized in Table 1 are normal once the 595 nm form has been accounted for, the interactions of ferricyanide-oxidized enzyme with H_2O_2 and with CO/O_2 are severely impaired.

Kinetic analysis of the reaction of bovine heart oxidase with H_2O_2 (Jünemann and Rich, unpublished results) showed that at least two spectrally similar, but not identical, **F**-type species, **F** and **F•**, are formed in addition to **P**, as is the case for the *bo*-type oxidase from *E. coli* (*26*). Briefly, for both bovine and *R. sphaeroides* oxidase, at alkaline pH, sequential reaction with two H_2O_2 molecules produces **P** and then **F**. At acidic pH, a different species, **F•**, can be generated by reaction with a single H_2O_2, possibly by fast, spontaneous decay of **P** or more likely by a direct conversion not involving a **P** intermediate.

The reaction kinetics of cytochrome oxidase from *R. sphaeroides* are similar to those of the bovine enzyme, and we have studied the H_2O_2 reaction of the E286 mutants over a range of H_2O_2 concentrations and pH values in order to probe formation of all three intermediates, **P**, **F•**, and **F**. Under no conditions could any **P** be detected in E286Q, either in equilibrium spectra or as transients. The reaction product, at a yield of no more than 25%, was invariably **F**-type, although the data did not allow us to distinguish between **F** and **F•**. Unless an extremely unstable **P** is invoked which does not accumulate due either to rapid reduction by a second H_2O_2 molecule or to fast spontaneous conversion to **F•** even at high pH, the simplest explanation is that **P** cannot be formed in the E286Q mutant enzyme and that the reaction with H_2O_2 produces **F•** with a wild-type rate constant for a pathway which does not involve a **P** intermediate. It is likely that the inability to form **P** is a major factor for the loss of activity in the peroxidase half-reaction with this mutant (*14*, *15*). These results also have implications for the

mechanism of H_2O_2 binding, since the residue E286 which is clearly very important for proton translocation appears also to be required in peroxide binding to form **P**. Although H_2O_2 itself is the kinetically active species and the net reaction formally involves binding of H_2O_2 (*38*), it may be that the peroxide bound at the binuclear center is an anionic form. Hence, protons originally on H_2O_2 would be lost while charge-compensating proton(s) required for the stable state would be concurrently taken up through a different route to bind at a different location, presumably at the "trap site" for pumped protons (cf. refs *4*, *9*), a process in which E286 would play a critical role. $\mathbf{F}^{\bullet}$ formation may involve protonation sites different from those involved in **P** formation, probably not requiring proton access through E286.

Incubation of cytochrome oxidase with CO/O_2 is an alternative method of generating **P** via a two-electron reduced mixed-valence enzyme. This reaction is inhibited significantly in E286Q, and also partially in E286D, in that the kinetics of **P** formation are slower than wild type in both mutants, with much reduced yields in E286Q. The spectrum of the reaction product is characteristic of **P** in the E286D form, but this is not the case for E286Q where some haem reduction is observed instead, presumably due to some electron redistribution. Incubation with CO under anaerobic conditions points to a defect in the reductive step, compatible with flow-flash data which suggest that the subsequent reaction of **R** with oxygen to form **P** is unaffected by the mutation (*10*, *12*). The results again suggest a role in the reduction of the binuclear center for protonatable groups whose access route for protons involves E286Q.

The Aerobic Steady State. The fraction of the E286Q enzyme that was not trapped in the unreactive 595 nm form could be reduced readily by dithionite. When monitored on a seconds time scale the kinetics of this reduction were similar to the wild-type enzyme and no block to electron transfer from haem *a* to haem a_3 could be detected. However, this reduction rate is very slow in comparison to turnover number (*39*) and is not a true reflection of viability of the equivalent catalytic step. The experiments presented in Figures 4 and 5 show that under aerobic steady-state conditions haem *a* is over 90% reduced while haem a_3 remains in the ferric state where formate (Figure 6b) and cyanide (Figure 6c) can be bound. Indeed, formate binding requires both haem a_3 and Cu_B to be oxidized (*24*). We conclude that net forward electron transfer from haem *a* to the binuclear center is impaired either kinetically or, since Ädelroth et al. (*12*) have shown that reverse electron transfer is unhindered, possibly for thermodynamic reasons, and that under steady-state conditions the major fraction of the E286Q enzyme which is not in the 595 nm form has a fully oxidized binuclear center.

Flow-flash data have indicated that the reaction of fully reduced oxidase with oxygen could not proceed beyond **P** on a millisecond time scale (*10*, *12*). However, there was no significant accumulation of oxygen intermediates, in particular **P**, under the steady-state conditions of the experiment shown in Figures 4 and 5 as judged from the position of the Soret peak and the Soret/α-band ratio in the steady state *minus* as prepared difference spectrum. Furthermore, the spectral changes following anaerobiosis (Figure 5A), ascribed solely to reduction of haem a_3 and some remaining haem *a*, are fully reversible on a seconds time scale by reintroduction of oxygen; that is, the state obtained following reintroduction of oxygen is spectrally identical to the steady state before anaerobiosis and is one in which haem *a* is reduced and haem a_3 is in the ferric oxidized **O** state. Hence, reduction of the binuclear center to the oxygen-reactive **R** state occurs at a limiting rate which prevents accumulation of oxygen intermediates. Neither is **P** accumulated during preparation or storage of the mutant enzyme as judged from the absolute spectra given in Figure 1. The two sets of results can be reconciled if, in addition to the **O** → **R** step, reaction steps after **P** formation are also inhibited. The flow-flash experiments (*10*, *12*) suggested that **P** → **F** and, possibly, **F** → **O** were inhibited. A time-resolved study of membrane potential generation also pointed to the possibility of an impaired **F** → **O** step in the E286Q mutant (*13*), although this conclusion may require verification since it is doubtful that the **F** state would have been formed on preincubation with H_2O_2.

In summary, the present and previous data lead to the conclusion that the E286Q mutation affects several steps in the catalytic cycle, namely **O** → **R**, **P** → **F** (*10*−*12*) and, possibly, **F** → **O** (*13*).

Coupling Mechanism. In E286Q, the lack of **P** or **F** species in the aerobic state indicates that, besides a role in the **P** → **F** and, possibly, the **F** → **O** steps, the conserved glutamate-286 is also required in the **O** → **P** transition. Since haem a_3 is predominantly ferric in the aerobic steady state, it may be concluded that it is the **O** → **R** step that is affected, a conclusion consistent with the observations in flow-flash experiments of a rapid **R** → **P** reaction in E286Q (*10*).

In the "glutamate trap" model for proton translocation in the haem/copper oxidases, the conserved glutamate is proposed to be involved in relocation of a charge-compensating proton to its "trap site" each time an electron is transferred from haem *a* to the binuclear center (*4*, *9*). Replacement of E286 by a nonprotonatable residue would be expected to hinder this proton relocation and, therefore, should hinder all steps involving electron transfer from haem *a* to the binuclear center. The conclusion that all steps discussed above are inhibited except **R** → **P** (the only one not requiring charge compensation by protonation) is consistent with such a role for E286.

However, the redox titrations of the reactive fraction of E286Q indicate that E286 is not one of the sites of net proton uptake associated with the reduction of haem *a* or Cu_B. This conclusion is consistent with FTIR data which indicate that the residue is protonated in both the oxidized and reduced states of the oxidase (*35*). Hence, its role may instead be to catalyze the transfer of protons which are redox-linked to haem *a*, perhaps located elsewhere in the D-channel, to the trap site (possibly located in the region of the haem propionates and nearby protonatable residues such as D407 and H411). In this case, deprotonation may be transient and energetically unfavorable. Catalysis of internal proton transfer might well be expected to involve bond rotations in E286, so that the proton is moved primarily as an integral part of the glutamic carboxylic acid. However, the effect of shortening the side chain by one carbon unit in E286D has a surprisingly small effect on turnover number in comparison to the wild type (Figure 1), suggesting that other mobile species (perhaps hydronium ions) are also involved in the proton-transfer process in this region.

Although the effects of the E286Q mutation are in accord with the glutamate trap proposal, several major questions remain. Most outstanding is the pathway by which additional substrate protons, H^+_S, reach the binuclear center to form water, a function suggested previously for the K-channel. However, the finding that only the **O** → **R** step is hindered by the K362M mutation is not at all consistent with this simple view since water formation, and hence H^+_S uptake, has generally been considered to be associated only with the **P** → **F** and **F** → **O** steps (*40*). It has been suggested that the K-channel may operate as an H^+_S channel only during part of the cycle (*13*), or may not be a channel at all (*16*). In either case, this raises the possibility of an additional role for the D-channel and E286 in some of the H^+_S transfer, although with the severe complication of how protons might be partitioned between the trap sites and the site of oxygen reduction. Recently, the restriction of proton translocation, and therefore of H^+_S transfer, solely to the **P** → **F** and **F** → **O** steps has been questioned (*6*). H^+_S transfer and proton translocation associated with **O** → **R**, as suggested in ref *6*, could provide an explanation of why mutations of both E286 and K362 impair this step, although the lack of effects of mutation K362M on subsequent steps still presents a puzzle. Studies of additional mutations at these and related sites will hopefully shed further light on these questions.

ACKNOWLEDGMENT

We thank Jonathan Ramsey for technical assistance and Prof. Robert Gennis (University of Urbana, Illinois) for supplying us with the *R. sphaeroides* strains and the purified enzyme preparations used in the initial stages of this project.

REFERENCES

1. Iwata, S., Ostermeier, C., Ludwig, B., and Michel, H. (1995) *Nature 376*, 660−669.
2. Tsukihara, T., Aoyama, H., Yamashita, E., Tomizaki, T., Yamaguchi, H., Shinzawa-Itoh, K., Nakashima, R., Yaono, R., and Yoshikawa, S. (1996) *Science 272*, 1136−1144.
3. Babcock, G. T., and Wikström, M. (1992) *Nature 356*, 301−309.
4. Rich, P. R. (1996) in *Protein Electron Transfer* (Bendall, D. S., Ed.) pp 217−248, BIOS Scientific Publishers Ltd., Oxford, U.K.
5. Rich, P. R., Meunier, B., Mitchell, R. M., and Moody, A. J. (1996) *Biochim. Biophys. Acta 1275*, 91−95.
6. Michel, H. (1998) *Proc. Natl. Acad. Sci. U.S.A. 95*, 12819−12824.
7. Hosler, J. P., Ferguson-Miller, S., Calhoun, M. W., Thomas, J. W., Hill, J., Lemieux, L., Ma, J., Georgiou, C., Fetter, J., Shapleigh, J., Tecklenburg, M. M. J., Babcock, G. T., and Gennis, R. B. (1993) *J. Bioenerg. Biomembr. 25*, 121−136.
8. Thomas, J. W., Lemieux, L. J., Alben, J. O., and Gennis, R. B. (1993) *Biochemistry 32*, 11173−11180.
9. Rich, P. R., Jünemann, S., and Meunier, B. (1998) *J. Bioenerg. Biomembr. 30*, 131−138.
10. Svensson-Ek, M., Thomas, J. W., Gennis, R. B., Nilsson, T., and Brzezinski, P. (1996) *Biochemistry 35*, 13673−13680.
11. Watmough, N. J., Katsonouri, A., Little, R. H., Osborne, J. P., Furlong-Nickels, E., Gennis, R. B., Brittain, T., and Greenwood, C. (1997) *Biochemistry 36*, 13736−13742.
12. Ädelroth, P., Svensson-Ek, M., Mitchell, D. M., Gennis, R. B., and Brzezinski, P. (1997) *Biochemistry 36*, 13824−13829.
13. Konstantinov, A. A., Siletsky, S., Mitchell, D., Kaulen, A., and Gennis, R. B. (1997) *Proc. Natl. Acad. Sci. U.S.A. 94*, 9085−9090.
14. Konstantinov, A. A., Vygodina, T., Capitanio, N., and Papa, S. (1998) *Biochim. Biophys. Acta 1363*, 11−23.
15. Vygodina, T. V., Pecoraro, C., Mitchell, D., Gennis, R., and Konstantinov, A. A. (1998) *Biochemistry 37*, 3053−3061.
16. Jünemann, S., Meunier, B., Gennis, R. B., and Rich, P. R. (1997) *Biochemistry 36*, 14456−14464.
17. Hosler, J. P., Shapleigh, J. P., Mitchell, D. H., Kim, Y., Pressler, M. A., Georgiou, C., Babcock, G. T., Alben, J. O., Ferguson-Miller, S., and Gennis, R. B. (1996) *Biochemistry 35*, 10776−10783.
18. Mitchell, D. M., and Gennis, R. B. (1995) *FEBS Lett. 368*, 148−150.
19. Hosler, J. P., Fetter, J., Tecklenburg, M. M. J., Espe, M., Lerma, C., and Ferguson-Miller, S. (1992) *J. Biol. Chem. 267*, 24264−24272.
20. Rich, P. R., and Moody, A. J. (1997) in *Bioelectrochemistry: principles and practice* (Gräber, P., and Milazzo, G., Eds.) pp 419−456, Birkhäuser Verlag AG, Basel, Switzerland.
21. Verkhovskaya, M. L., García-Horsman, A., Puustinen, A., Rigaud, J.-L., Morgan, J. E., Verkhovsky, M. I., and Wikström, M. (1997) *Proc. Natl. Acad. Sci. U.S.A. 94*, 10128−10131.
22. Mitchell, D. M., Aasa, R., Ädelroth, P., Brzezinski, P., Gennis, R. B., and Malmström, B. G. (1995) *FEBS Lett. 374*, 371−374.
23. Liao, G. L., and Palmer, G. (1996) *Biochim. Biophys. Acta Bio-Energetics 1274*, 109−111.
24. Kojima, N., and Palmer, G. (1983) *J. Biol. Chem. 258*, 14908−14913.
25. Fabian, M., and Palmer, G. (1995) *Biochemistry 34*, 13802−13810.
26. Brittain, T., Little, R. H., Greenwood, C., and Watmough, N. J. (1996) *FEBS Lett. 399*, 21−25.
27. Bickar, D., Bonaventura, C., and Bonaventura, J. (1984) *J. Biol. Chem. 259*, 10777−10783.
28. Meunier, B., and Rich, P. R. (1997) in *Oxygen Homeostasis and Its Dynamics* (Ishimura, Y., Shimada, H., and Suematsu, M., Eds.) pp 106−111, Springer-Verlag, Tokyo, Japan.
29. Moody, A. J., and Rich, P. R. (1990) *Biochim. Biophys. Acta 1015*, 205−215.
30. Meunier, B., Ortwein, C., Brandt, U., and Rich, P. R. (1998) *Biochem. J. 330*, 1197−1200.
31. Orii, Y. (1988) *Ann. N. Y. Acad. Sci. 550*, 105−117.
32. Chance, B., Saronio, C., and Leigh, J. S. (1975) *J. Biol. Chem. 250*, 9226−9237.
33. Babcock, G. T., Jean, J. M., Johnston, L. N., Palmer, G., and Woodruff, W. H. (1984) *J. Am. Chem. Soc. 106*, 8305−8306.
34. Zhen, Y., Qian, J., Follmann, K., Hayward, T., Nilsson, T., Dahn, M., Hilmi, Y., Hamer, A. G., Hosler, J. P., and Ferguson-Miller, S. (1998) *Protein Expression Purif. 13*, 326−336.
35. Puustinen, A., Bailey, J. A., Dyer, R. B., Mecklenburg, S. L., Wikström, M., and Woodruff, W. H. (1997) *Biochemistry 36*, 13195−13200.
36. Ortwein, C., Link, T. A., Meunier, B., Colson, A., Rich, P. R., and Brandt, U. (1997) *Biochim. Biophys. Acta 1321*, 79−92.
37. Ostermeier, C., Harrenga, A., Ermler, U., and Michel, H. (1997) *Proc. Natl. Acad. Sci. U.S.A. 94*, 10547−10553.
38. Mitchell, R., and Rich, P. R. (1994) *Biochim. Biophys. Acta 1186*, 19−26.
39. Brunori, M., Giuffre, A., D'Itri, E., and Sarti, P. (1997) *J. Biol. Chem. 272*, 19870−19874.
40. Wikström, M. (1989) *Nature 338*, 776−778.

BI9830112